Supplementary information: Autolysin-mediated peptidoglycan hydrolysis is required for the surface display of *Staphylococcus aureus* cell wall-anchored proteins

Allison C. Leonard[1], Mariya I. Goncheva[2†], Stephanie E. Gilbert[1], Hiba Shareefdeen[1], Laurenne E. Petrie[1], Laura K. Thompson[1], Cezar M. Khursigara[1], David E. Heinrichs[2] & Georgina Cox[1*]

[1]College of Biological Sciences, Department of Molecular and Cellular Biology, University of Guelph, 50 Stone Rd E, Guelph, Ontario, Canada N1G 2W1

[2]Department of Microbiology and Immunology, University of Western Ontario, London, Ontario, Canada N6A 5C1

†Present address: Department of Biochemistry and Microbiology, University of Victoria, Victoria, British Columbia, Canada V8P 5C2

[*]Corresponding author: Dr. Georgina Cox, College of Biological Sciences, Department of Molecular and Cellular Biology, University of Guelph, 50 Stone Rd E, Guelph, Ontario, Canada N1G 2W1. Tel: +1 519-824-4120, Email: gcox@uoguelph.ca

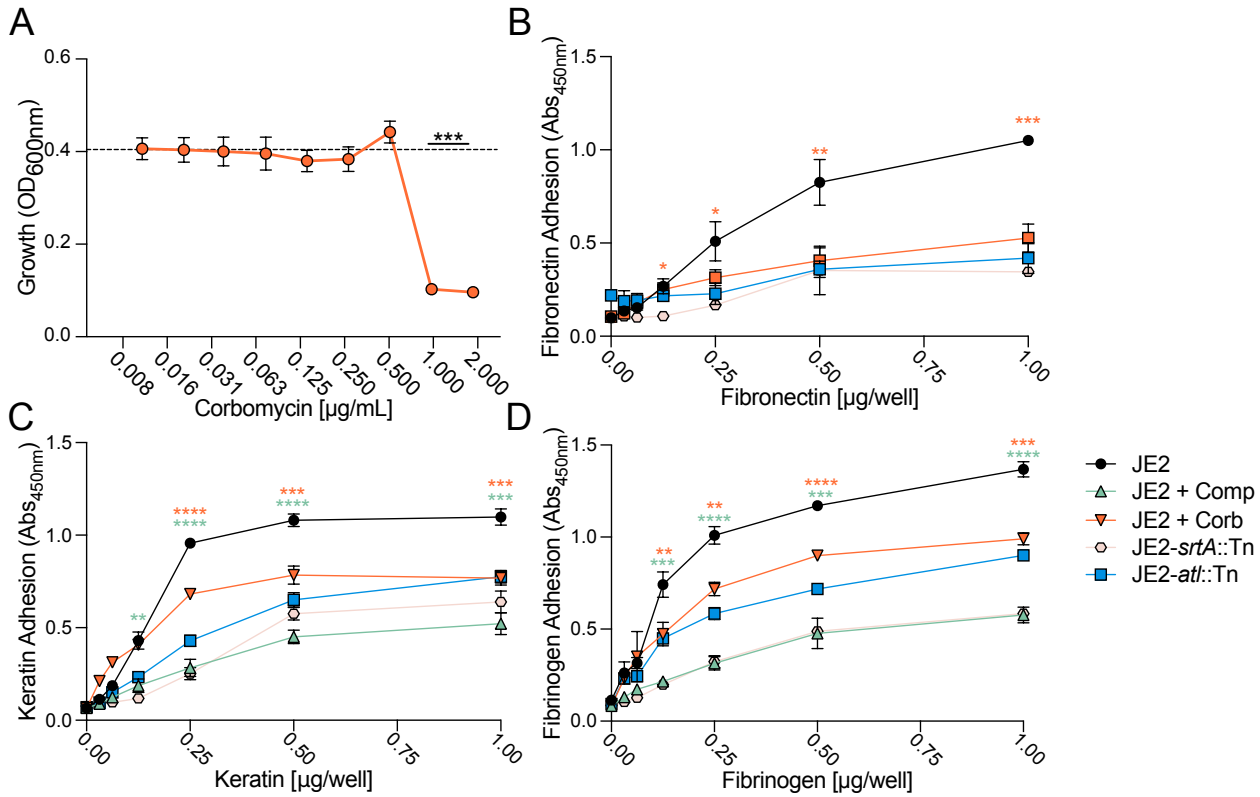

Fig. S1. Complestatin and corbomycin inhibit MRSA USA300 (JE2) adhesion to fibronectin, keratin, and fibrinogen. (A) End-point readings to assess the growth (OD_{600nm}) of JE2 in the presence of corbomycin. Each data point represents the average of three biological replicates ± the standard deviation, and each biological replicate is the mean of eight technical replicates. The average of 24 replicates of JE2 grown in the presence of 1% DMSO (*v/v*) as a solvent control represents growth in the absence of corbomycin (dashed black line). Corbomycin adhesion assays were performed at concentrations that were sub-inhibitory (≤0.5 ug/mL) for growth (OD_{600nm}), as determined by statistical analysis and comparison to the solvent control. **(B)** Fibronectin, **(C)** keratin, and **(D)** fibrinogen ELISA-based adhesion assays (Abs_{450nm}) of complestatin- (0.5 µg/mL) and corbomycin-treated (0.5 µg/mL) cells. Isogenic sortase A (*srtA*::Tn) and Atl (*atl*::Tn) transposon mutants were included as adhesion-defective controls. Each data point represents the average of three biological replicates ± the standard deviation. *P*-values were calculated using the two-tailed unpaired Student's t-test. Statistically significant decreases in adhesion in the presence of complestatin (green asterisk) and corbomycin (orange asterisk) compared to JE2 are denoted as $P \leq 0.05$*; $P \leq 0.01$**; $P \leq 0.001$***, $P \leq 0.0001$****. Related to Figure 1.

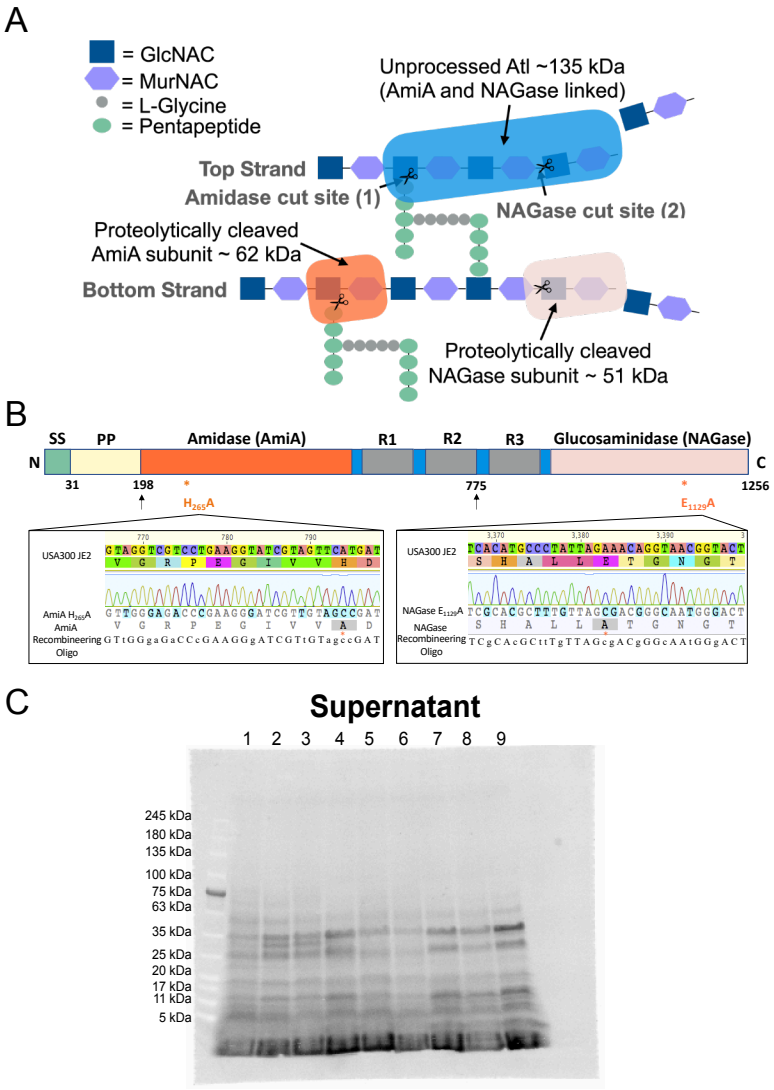

Fig. S2. Schematic diagram depicting the processing of *S. aureus* peptidoglycan by Atl. (A) Atl (blue), AmiA (orange), and NAGase (pink) process the peptidoglycan at distinct sites. On the top strand, AmiA initially hydrolyses crosspeptides leaving the peptidoglycan strand exposed for NAGase to cleave between GlcNAc and MurNAc. On the bottom strand, proteolytically cleaved AmiA and NAGase subunits work independently to degrade the remaining cell wall (1). **(B)** Schematic diagram of Atl domain organization and catalytic mutant generation. Amino acid numbering is shown, and key catalytic active site residues are labeled red; the panel below shows Sanger sequencing of the genome editing, where the active site residue of AmiA ($H_{265}A$; highlighted in grey) and NAGase ($E_{1129}A$, highlighted grey) were mutagenized. Additional introduced mutations (highlighted in cyan) are silent and were introduced to remove the PAM and improve recombineering efficiency. SS = signal peptide; PP = propeptide of unknown function; R1-R3 = repeated sequence domains. **(C)** Representative (single technical replicate) of

total protein Stain Free (Biorad) images used for AmiA normalization of the supernatant fraction (Fig. 2B). Samples 1-3: JE2-Δ*spa* Δ*sbi* biological replicates 1-3; samples 4-6: JE2-*atl*::Tn biological replicates 1-3; samples 7-9: JE2-*atl* H265A_E1129A Δ*spa*Δ*sbi* biological replicates 1-3.

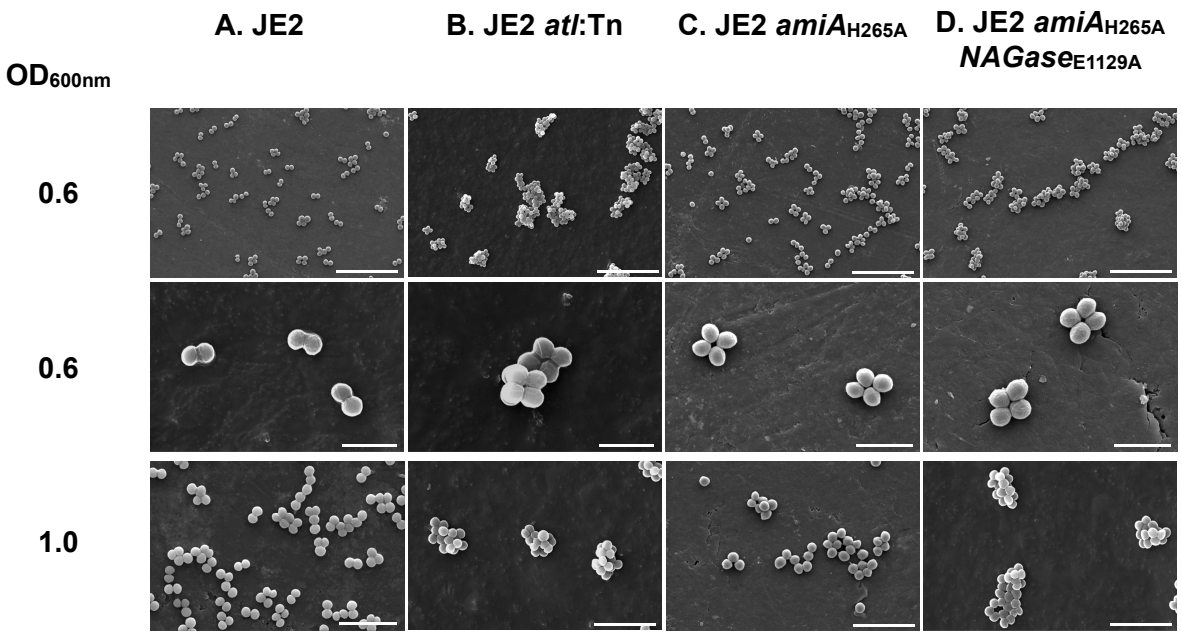

Fig. S3. Scanning electron microscopy analysis of autolysin (Atl)-deficient *S. aureus.* (A) MRSA USA300 JE2; **(B)** JE2-*atl*::Tn; **(C)** JE2-*atl* $H_{265}A$; **(D)** JE2-*atl* $H_{265}A\_E_{1129}A$. The strains were sampled at different stages of the growth cycle (OD_{600nm}).

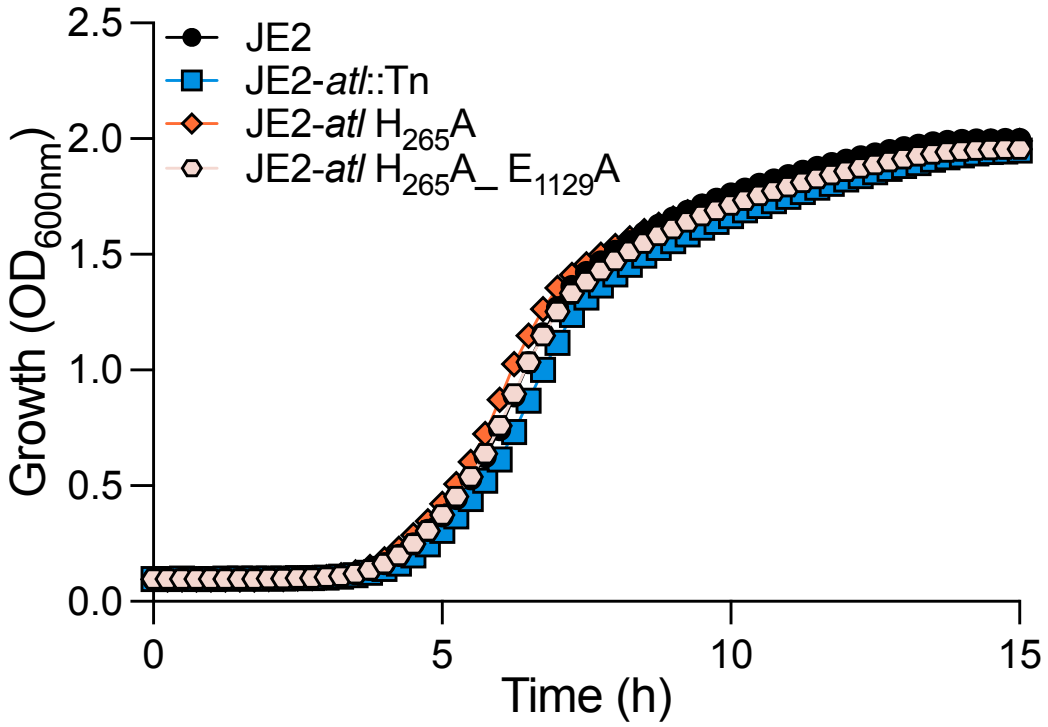

Fig. S4. Growth profiling of autolysin (*atl*) inactivated mutant strains compared to the wild-type MRSA USA300 JE2 strain. Data points represent the mean of 24 technical replicates.

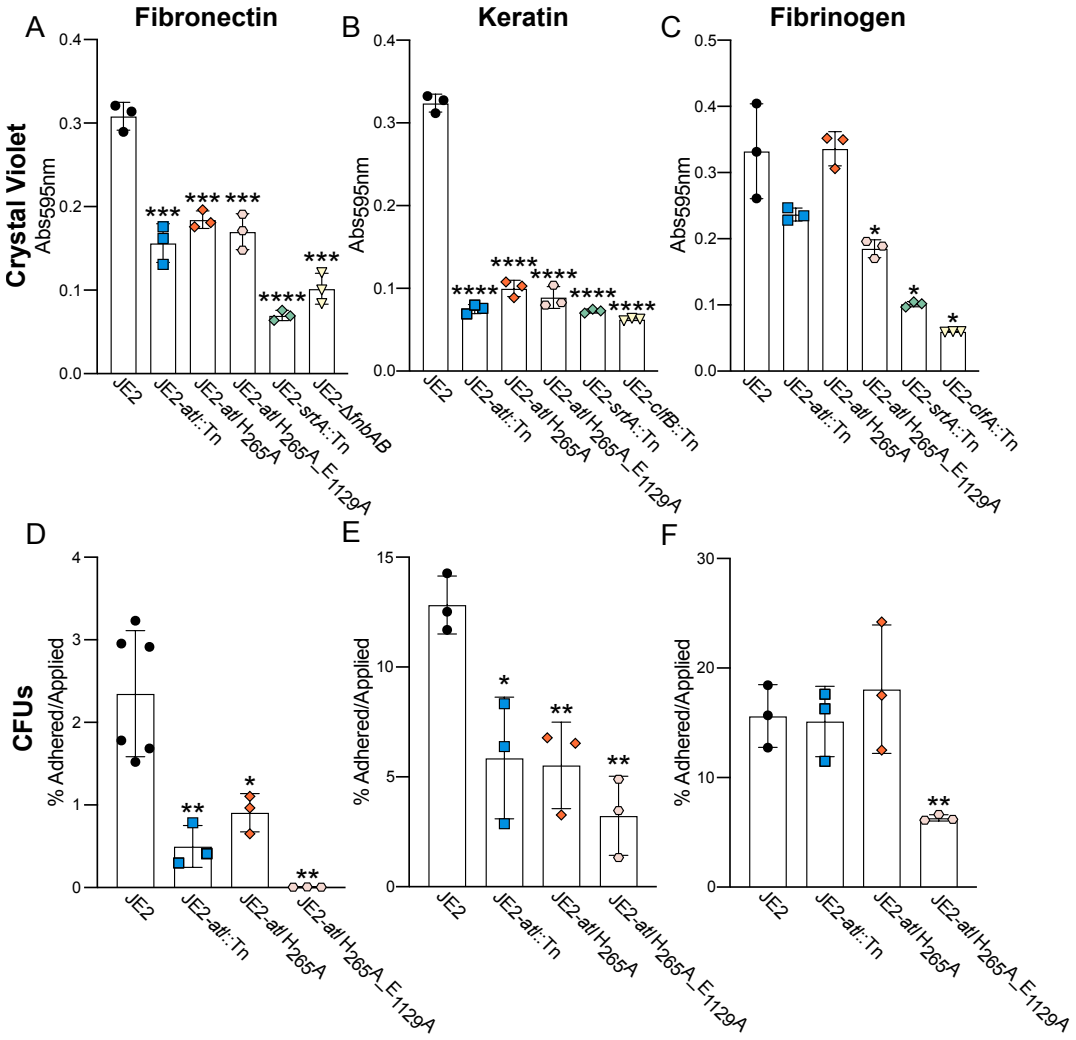

Fig. S5. Autolysin (Atl) catalytic function is required for *S. aureus* adhesion to host ligands. Crystal violet detection of MRSA USA300 JE2 (JE2) adhesion to **(A)** fibronectin (0.5 µg/well), **(B)** keratin (0.125 µg/well), and **(C)** fibrinogen (0.25 µg/well). Manual enumeration of applied and adhered colony forming units (CFUs) assessing adhesion to **(D)** fibronectin (0.25 µg/well), **(E)** keratin (0.125 µg/well), and **(F)** fibrinogen (0.0625 µg/well). Each data point represents the average of three biological replicates ± the standard deviation. For CFUs each biological replicate is the average of three technical replicates. *P*-values were calculated using the two-tailed unpaired Student's *t*-test comparing each mutant to JE2. Statistically significant decreases in adhesion compared to JE2 were denoted as $P \leq 0.05$ *, $P \leq 0.01$**$P \leq 0.001$***, $P \leq 0.0001$****. Related to Fig. 2.

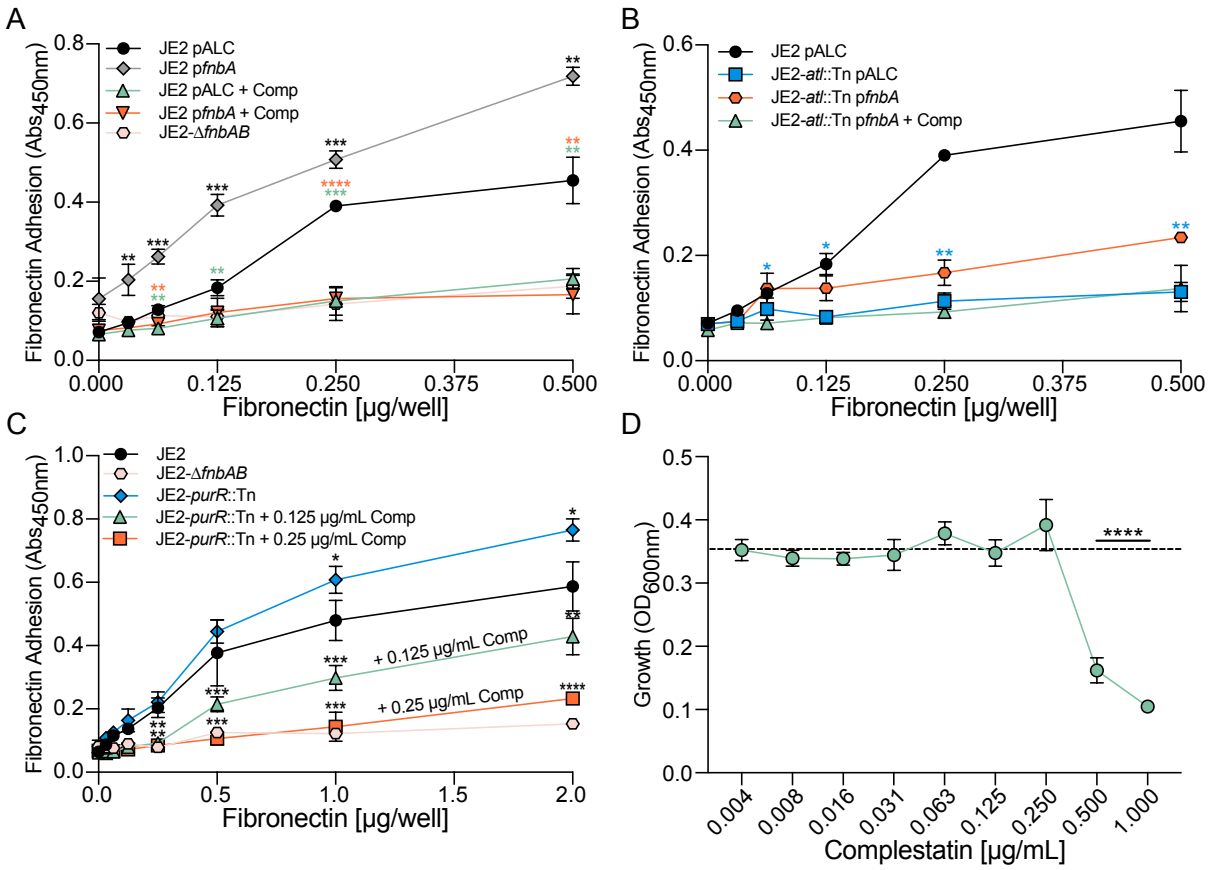

Fig. S6. The overexpression of cell wall-anchored adhesins did not restore adhesion in autolysin-defective cells (A) ELISA-based fibronectin adhesion assays (Abs_{450nm}) of JE2 pALC2073:*fnbA* (labeled p*fnbA*) and the wild-type strain (JE2 pALC2073) in the presence and absence of complestatin (0.5 µg/mL). A mutant devoid of the FnBPs was included as an adhesion defective control (JE2-Δ*fnbAB*). **(B)** ELISA-based fibronectin adhesion assays (Abs_{450nm}) of JE2-*atl*::Tn pALC2073:*fnbA* (labeled p*fnbA*) and the wild-type strain (JE2-*atl*::Tn pALC2073) in the presence and absence of complestatin (0.5 µg/mL). **(C)** ELISA-based fibronectin adhesion assay of JE2-*purR*::Tn in the presence and absence of complestatin (0.125 and 0.25 µg/mL). **(D)** End-point readings to assess the growth (OD_{600nm}) of JE2-*purR*::Tn in the presence of complestatin. Each data point represents the average of three biological replicates ± the standard deviation, where each biological represents the mean of eight technical replicates. The dashed black line is the mean of 24 replicates of JE2-*purR*::Tn grown in the presence of 1% DMSO as a solvent control. Adhesion assays were performed at complestatin concentrations that were sub-inhibitory (≤0.25 µg/mL) for growth, as determined by statistical analysis and comparison to the solvent control. For the adhesion assays, each data point represents the average of at least three biological replicates ± the standard deviation. All *P*-values were calculated using the two-tailed unpaired Student's

t-test. Statistically significant decreases in adhesion/growth are denoted as $P \leq 0.05$*; $P \leq 0.01$**; $P \leq 0.001$***; $P \leq 0.0001$****.

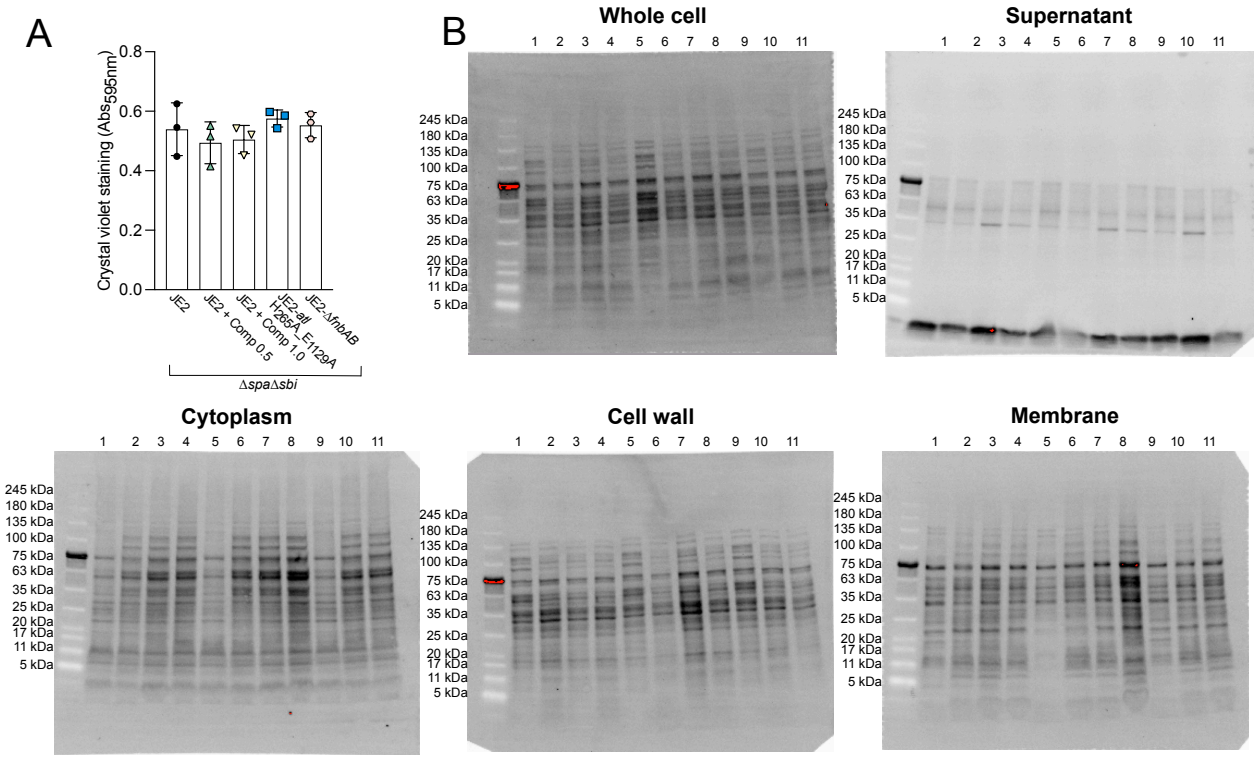

Fig. S7. Microtiter plate adhesion and immunoblot blot total protein controls associated with Fig. 3. **(A)** Crystal violet staining (Abs_{595nm}) of immobilized whole cells on the surface of microtiter plates for the detection of surface exposed FnBPs. **(B)** Representative (single technical replicate) of total protein Stain Free (Biorad) images used for protein quantification for the whole cell, supernatant, cytoplasm, cell wall, and membrane fractions. (1) JE2-Δ*spa*Δ*sbi* biological replicate 1, (2) JE2-Δ*spa*Δ*sbi* + Comp biological replicate 1, (3) JE2-*atl* H265A_E1129A Δ*spa*Δ*sbi* biological replicate 1, (4) JE2-Δ*fnbAB*Δ*spa*Δ*sbi* biological replicate 1, (5) JE2-Δ*spa*Δ*sbi* biological replicate 1, (6) JE2-Δ*spa*Δ*sbi* + Comp biological replicate 2, (7) JE2-*atl* H265A_E1129A Δ*spa*Δ*sbi* biological replicate 2, (8) JE2-Δ*fnbAB*Δ*spa*Δ*sbi* biological replicate 2, (9) JE2-Δ*spa*Δ*sbi* biological replicate 3, (10) JE2-Δ*spa*Δ*sbi* + Comp biological replicate 3, (11) JE2-*atl* H265A_E1129A Δ*spa*Δ*sbi* biological replicate 3. Related to Fig. 3.

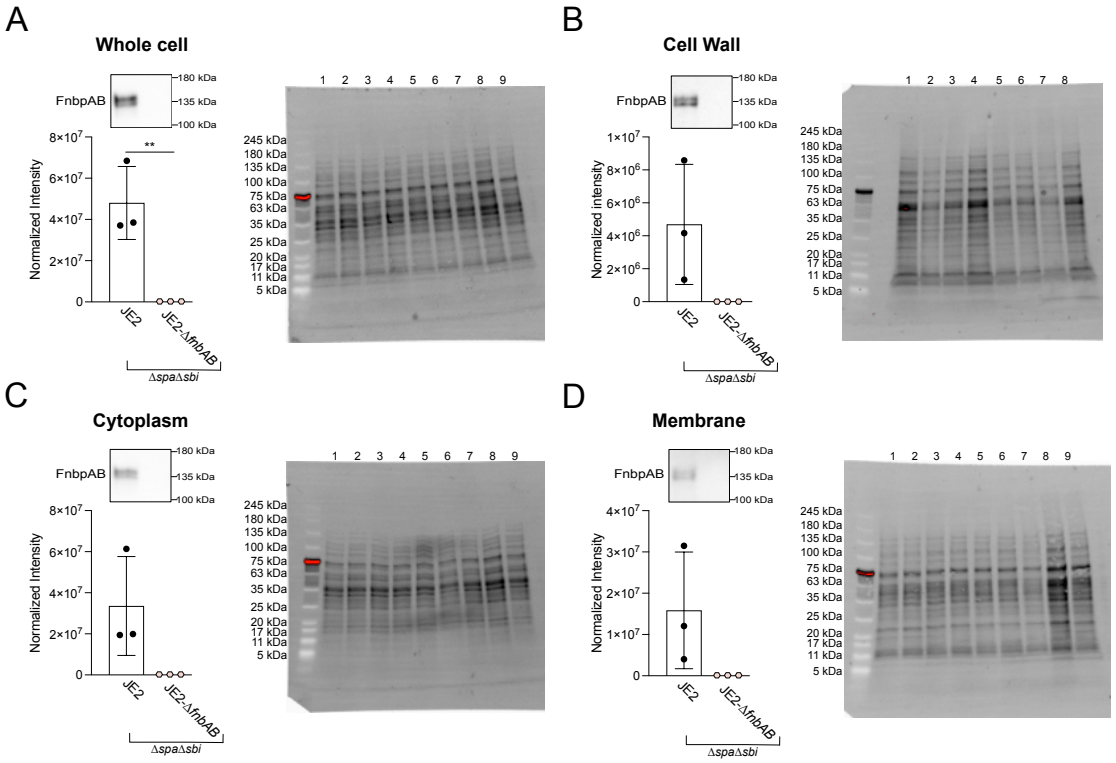

Fig. S8. **Assessing the cellular localization of the FnBPs in MRSA USA300 JE2.** Immunoblot analysis of the FnBPs in **(A)** whole cell, **(B)** cell wall, **(C)** cytoplasm and **(D)** membrane fractions. The total protein Stain Free (Biorad) image used for protein quantification is shown adjacent to each fraction. (1) JE2-*srtA*::Tn Δ*spa*Δ*sbi* biological replicate 1, (2) JE2-Δ*spa*Δ*sbi* biological replicate 1, (3) JE2-Δ*fnbAB*Δ*spa*Δ*sbi* biological replicate 1, (4) JE2-*srtA*::Tn Δ*spa*Δ*sbi* biological replicate 2, (5) JE2-Δ*spa*Δ*sbi* biological replicate 2, (6) JE2-Δ*fnbAB*Δ*spa*Δ*sbi* biological replicate 2, (7) JE2-*srtA*::Tn Δ*spa*Δ*sbi* biological replicate 3, (8) JE2-Δ*spa*Δ*sbi* biological replicate 3, (9) JE2-Δ*fnbAB*Δ*spa*Δ*sbi* biological replicate 3. For each immunoblot, data points represent a single biological replicate ± the standard deviation. Representative immunoblots from one biological replicate are shown. *P*-values were calculated using the two-tailed unpaired Student's *t*-test comparing each mutant to the wild-type strain (JE2). Statistically significant decreases in adhesion and normalized intensity compared to JE2 were denoted as $P \leq 0.01$**. Protein abundance was normalized to total protein using a stain free approach. Associated with Fig. 3 and Fig S7.

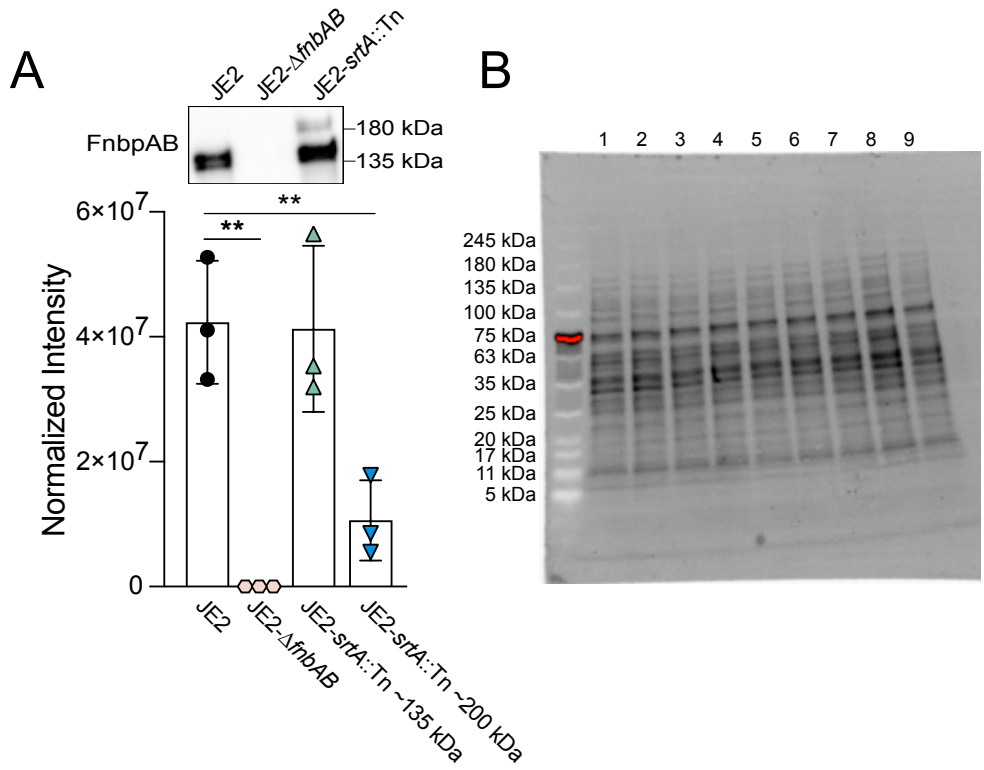

Fig S9. Assessing FnBPs in a sortase A (*srtA*) inactivated MRSA USA300 JE2 mutant (JE2-*srtA*::Tn). (A) Immunoblot analysis of the FnBPs in whole cell lysates. **(B)** Representative total protein Stain Free (Biorad) image used for protein quantification. (1) JE2-*srtA*::Tn Δ*spa*Δ*sbi* biological replicate 1, (2) JE2-Δ*spa*Δ*sbi* biological replicate 1, (3) JE2-Δ*fnbAB*Δ*spa*Δ*sbi* biological replicate 1, (4) JE2-*srtA*::Tn Δ*spa*Δ*sbi* biological replicate 2, (5) JE2-Δ*spa*Δ*sbi* biological replicate 2, (6) JE2-Δ*fnbAB*Δ*spa*Δ*sbi* biological replicate 2, (7) JE2-*srtA*::Tn Δ*spa*Δ*sbi* biological replicate 3, (8) JE2-Δ*spa*Δ*sbi* biological replicate 3, (9) JE2-Δ*fnbAB*Δ*spa*Δ*sbi* biological replicate 3. For each immunoblot, data points represent the average of three technical replicates for a single biological replicate ± the standard deviation. Representative immunoblots from one biological replicate are shown. *P*-values were calculated using the two-tailed unpaired Student's *t*-test comparing each mutant to the wild-type strain (JE2). Statistically significant decreases in adhesion and normalized intensity compared to JE2 were denoted as $P \leq 0.01$**. Protein abundance was normalized to total protein using a stain free approach.

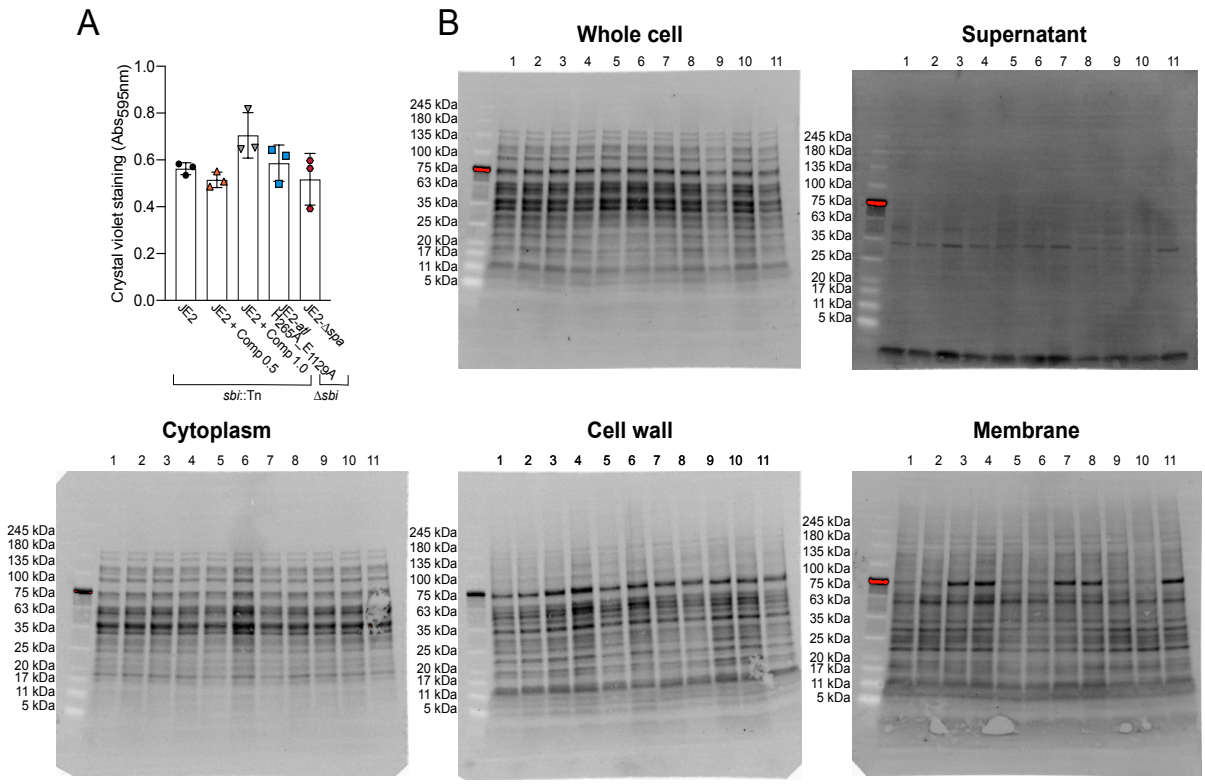

Fig. S10. Microtiter plate adhesion and immunoblot blot total protein controls associated with Fig. 4. (A) Crystal violet staining (Abs_{595nm}) of immobilized whole cells on the surface of microtiter plates for the detection of surface exposed Spa. **(B)** Representative (single technical replicate) of total protein Stain Free (Biorad) images used for protein quantification of whole cell, supernatant, cytoplasm, cell wall, and membrane fractions. (1) JE2-*sbi*::Tn biological replicate 1, (2) JE2-*sbi*::Tn + Comp biological replicate 1, (3) JE2-*atl* H265A_E1129A Δ*sbi* biological replicate 1, (4) JE2-Δ*spa*Δ*sbi* biological replicate 1, (5) JE2-*sbi*::Tn biological replicate 2, (6) JE2-*sbi*::Tn + Comp biological replicate 2, (7) JE2-*atl* H265A_E1129A Δ*sbi* biological replicate 2, (8) JE2-Δ*spa*Δ*sbi* biological replicate 2, (9) JE2-*sbi*::Tn biological replicate 3, (10) JE2-*sbi*::Tn + Comp biological replicate 3, (11) JE2-*atl* H265A_E1129A Δ*sbi* biological replicate 3, JE2-Δ*spa*Δ*sbi* biological replicate 3. Related to Fig.4.

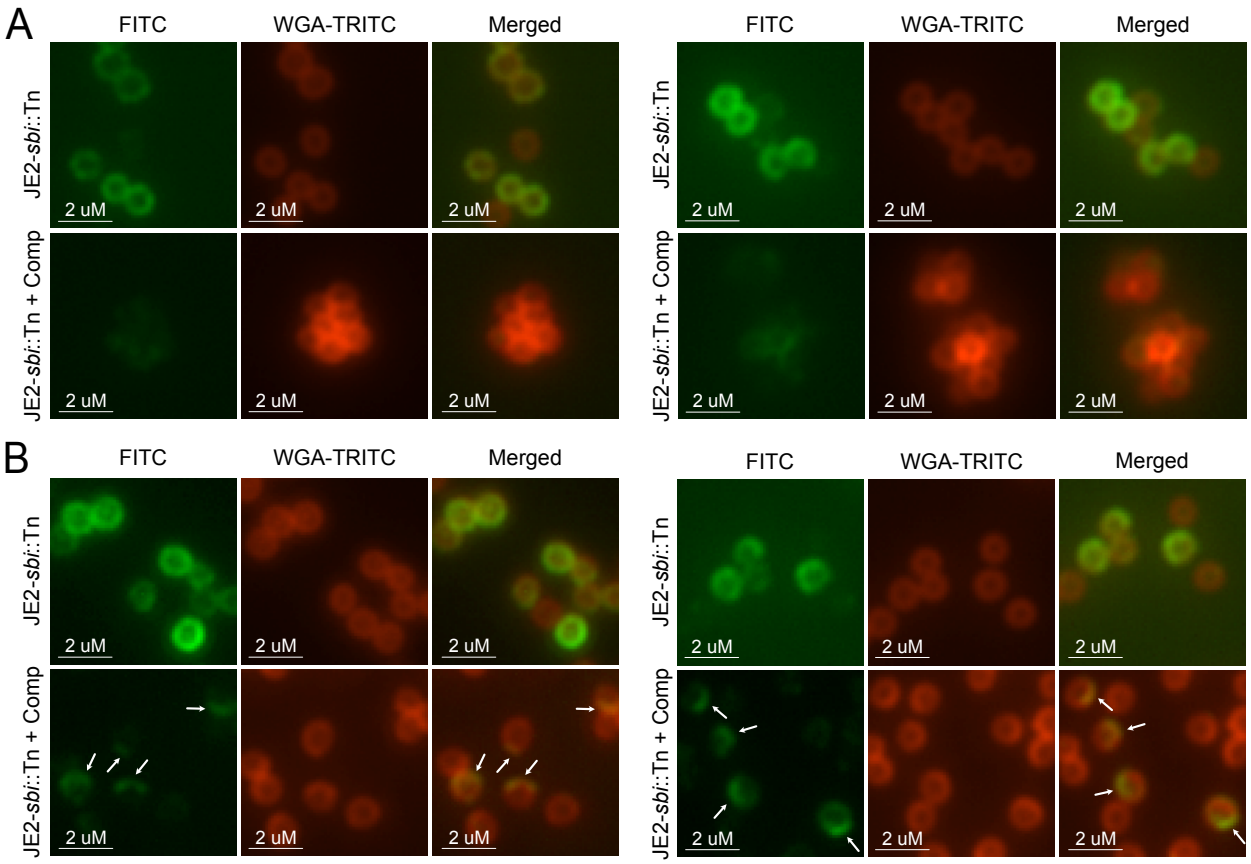

Fig. S11. Immunofluorescence microscopy analysis of complestatin-treated cells. Two further biological replicates assessing Spa localization in the presence of complestatin **(A)** pre- and **(B)** post-sonication. The arrows indicate Spa concentrated on one face of the separated cells. Related to Fig 5.

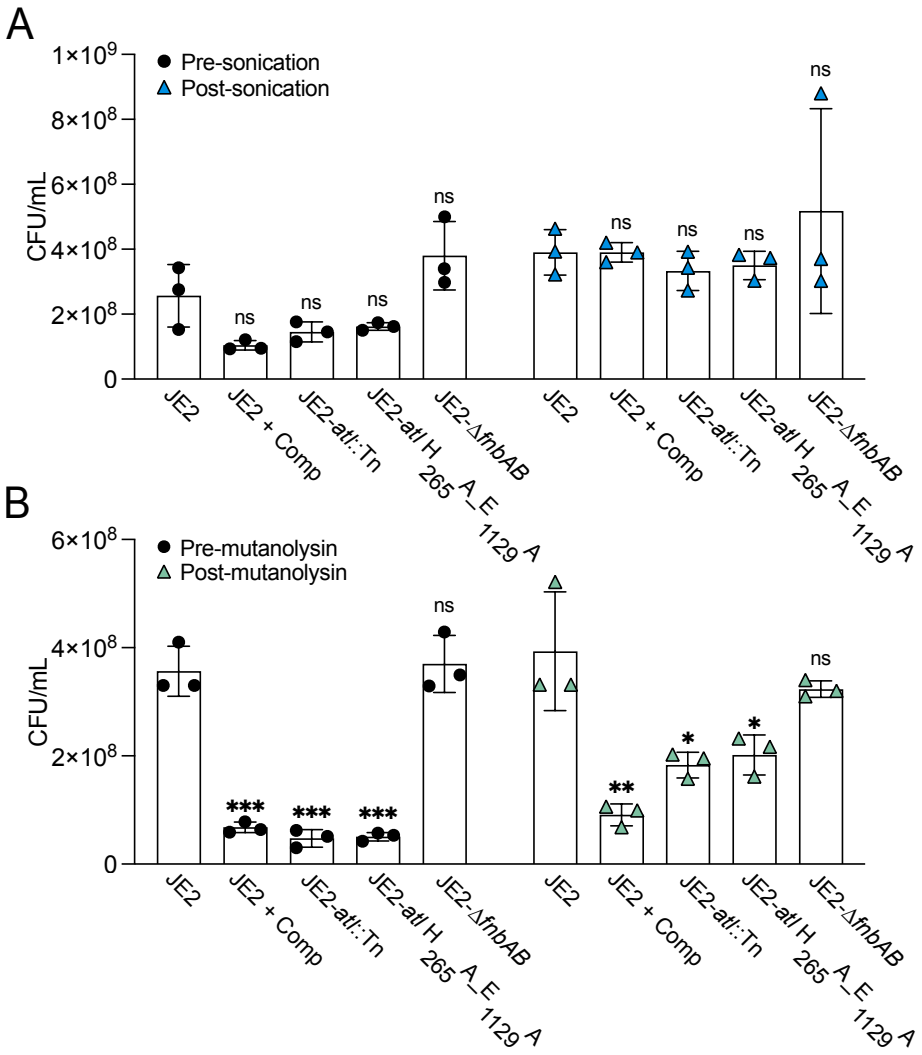

Fig. S12. Viability following mechanical and enzymatic separation of autolysin-associated cell clusters. Measurement of the CFU/mL of each strain **(A)** pre-sonication (black) and post-sonication (blue) and **(B)** pre-mutanolysin (black) and post-mutanolysin (green) treatment. Each data point represents the average of three biological replicates ± the standard deviation. The CFU/mL for each sample increased after sonication and mutanolysin treatment due to separation of the autolysin-associated cells clusters. *P*-values were calculated using the two-tailed unpaired Student's *t*-test comparing each mutant to JE2. Statistically significant differences were denoted as $P \leq 0.05$*, $P \leq 0.01$**, $P \leq 0.001$***.

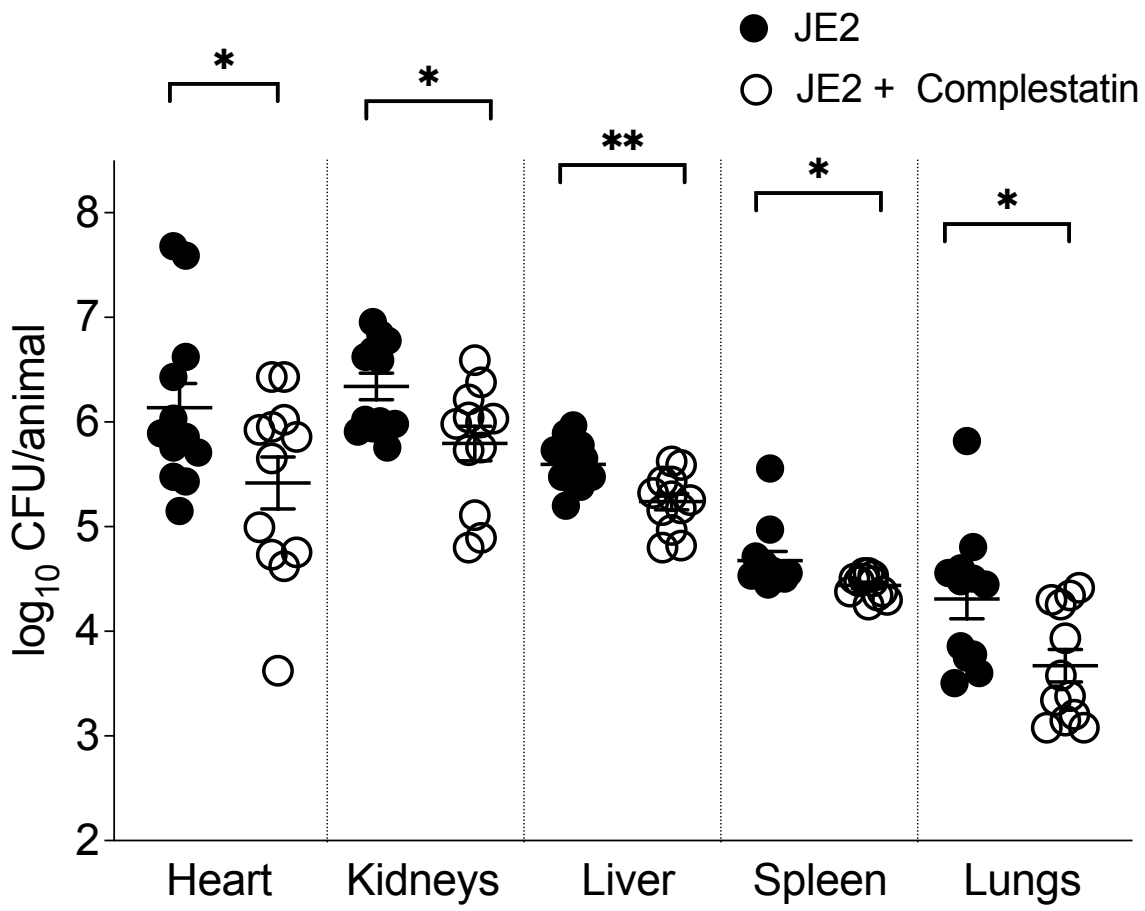

Figure S13. Complestatin exhibits antivirulence properties. Complestatin (0.5 µg/mL) significantly reduced the bacterial burden in all organs at 24 h post-infection (hpi). Data points represent each animal, and the lines are the mean ± the standard error. **P*-value < 0.05, ***P*-value < 0.01, based on a Student's unpaired *t*-test.

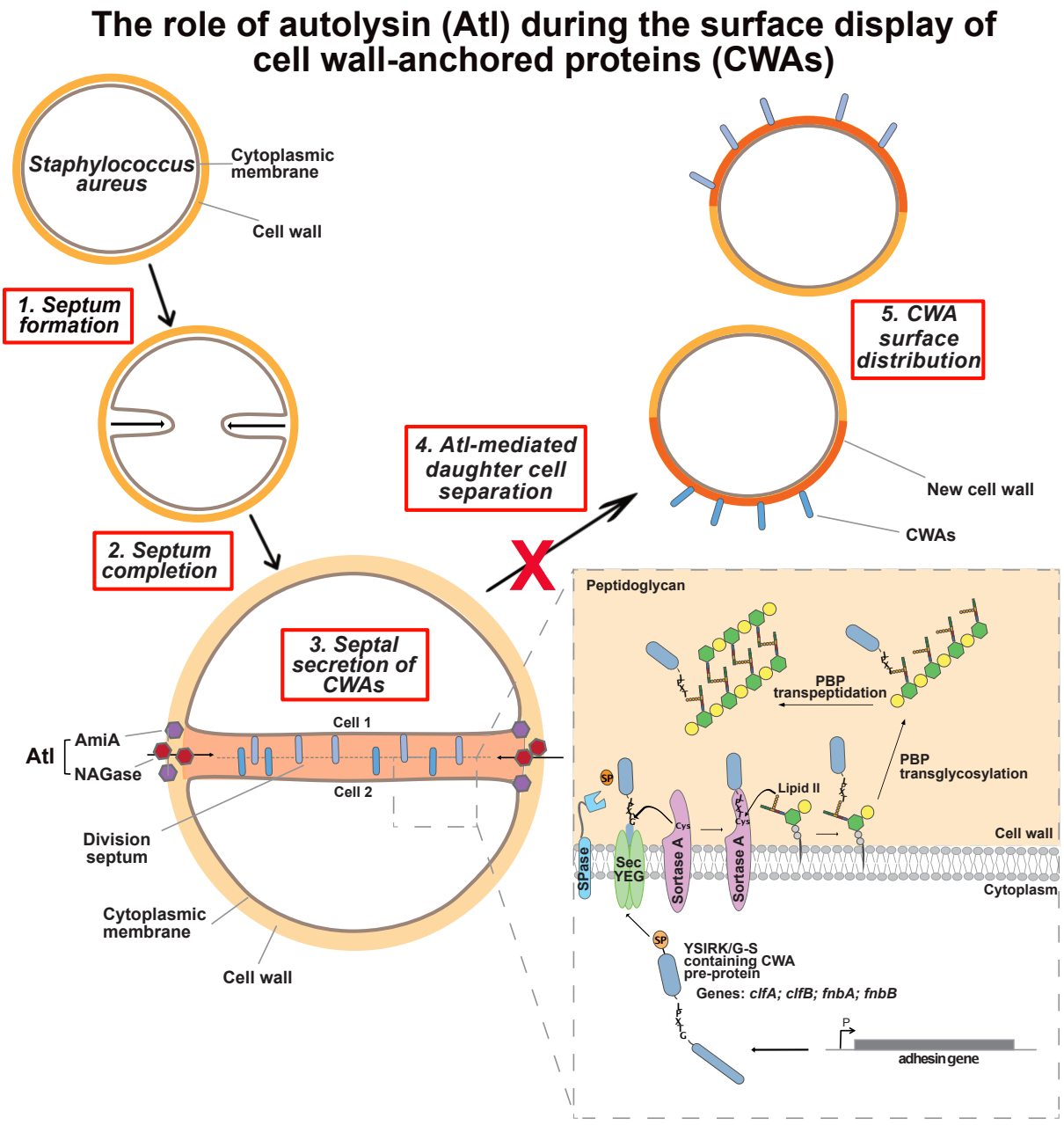

Fig. S14. Schematic representation of the septal secretion of CWA proteins. Atl loss-of-function (represented as a red X) causes septal sequestration and occlusion of CWA proteins, reducing the overall surface levels of these proteins.

Table S1. Strains and plasmids used in this study

Strain/Plasmids	Description	Source
Strains		
S. aureus		
USA300 JE2	USA300 strain LAC cured of resistance plasmids, CA-MRSA	BEI Resources; (2)
JE2-Δ*fnbAB*	USA300 JE2 devoid of fibronectin-binding proteins A and B	(3)
JE2-*srtA*::Tn	USA300 JE2 with a transposon insertion in the *srtA* gene, Ery^r	BEI Resources; (2)
JE2-*clfB*::Tn	USA300 JE2 with a transposon insertion in the *clfB* gene, Ery^r	(4)
JE2-*atl*::Tn	USA300 JE2 with a transposon insertion in the *atl* gene, Ery^r	(4)
JE2-*sbi*::Tn	USA300 JE2 with a transposon insertion in the *sbi* gene, Ery^r	BEI Resources; (2)
JE2-*purR*::Tn	USA300 JE2 with a transposon insertion in the *purR* gene, Ery^r	BEI Resources; (2)
JE2-*atl* $H_{265}A$	USA300 JE2 with a $H_{265}A$ substitution in the *atl* gene	This study
JE2-*atl* $H_{265}A\_E_{1129}A$	USA300 JE2 with a $H_{265}A$ and $E_{1129}A$ substitution in the *atl* gene	This study
JE2-*atl* $H_{265}A\_E_{1129}A$ Δ*sbi*	USA300 JE2 with a $H_{265}A$ and $E_{1129}A$ substitution in the *atl* gene and devoid of *sbi* gene	This study
JE2-Δ*spa*Δ*sbi*	USA300 JE2 devoid of *sbi* and *spa* genes	(3)
JE2-*atl*::Tn Δ*spa*Δ*sbi*	USA300 JE2-*atl*::Tn devoid of *sbi* and *spa* genes, Ery^r	This study
JE2-*atl* $H_{265}A\_E_{1129}A$ *ΔspaΔsbi*	USA300 JE2-*atl*-AmiA $H_{265}A$/NAGase $E_{1129}A$ devoid of *sbi* and *spa* genes	This study
JE2-*ΔfnbAB* Δ*spa*Δ*sbi*	USA300 JE2 *ΔfnbAB* devoid of *sbi* and *spa* genes	This study
RN4220	Inactivated restriction-modification system, capable of accepting foreign DNA	(5, 6)

E. coli

DH5α	endA- routine cloning host for high quality DNA preparations	ThermoFisher Scientific
IM08B	*S. aureus* methylation machinery, SA08BWPN25-hsdS (CC8-1) (SAUSA300_0406) of NRS384 integrated between the essQ and cspB	BEI Resources; (7)
Plasmids		
pJB38	Cam^r, pCL10 with Pxyl/tetO-secY570 and XhoI site removed, temperature sensitive	BEI Resources; (8)
pTnT	Ery^r, pJB38 with homologous DNA to *Bursa aurealis*, temperature sensitive	BEI Resources; (8)
pCas9counter	Ery^r, expresses modifiable sgRNA and cas9, temperature sensitive	(9)
pCas9counter:sgRNA_AmiA	Ery^r, sgRNA designed to target PAM near AmiA H265 in JE2-atl	This study
pCas9counter:sgRNA_NAGase	Ery^r, sgRNA designed to target PAM near NAGase E1129 in JE2-atl	This study
pCN-EC2132tet	Cam^r, expresses recombinase EF2132 for incorporating ssDNA oligonucleotides into USA300 genome, temperature sensitive	(9)
pALC2073	Amp^r, multicopy shuttle vector with a TetR-inducible Pxyl/tetO promoter	(10)
pALC2073:*fnbpA*	Amp^r, Atc inducible *E. coli-S. aureus* shuttle vector, expressing *fnbpA* from USA300	(3)

Ery^r, erythromycin resistance; Cam^r, chloramphenicol resistance; Amp^r, ampicillin resistance

Table S2. Primers and oligonucleotides used in this study

Primers/Oligonucleotides	Sequence (5' - 3')	Source
Primers used in this study		
AmiA_F_check	CCGTTGGTGCTGTTTC	This study
AmiA_R_check	GCTGCAACTACATCAG	This study
NAGase_F_check	CACCACCAACGATTG	This study
NAGase_R_check	CGCTTAGACCAACCA	This study
Atl_FullFwd_Check	GTTAACCTCGCTTAATTA	This study
Atl_FullRvs_Check	CGTTGTAACACGACAATAG	This study
Atl_Check_1	CATATTCAATCAAACCTGG	This study
Atl_Check_2	GGTGCAGTTAAATCTTTTGC	This study
Atl_Check_3	GATTACATTCGTAAAAATAAC	This study
Atl_Check_4	ATTATTTGTTGTAGGTGTTG	This study
Atl_Check_5	TAGAAATATTTTGTGGTTG	This study
Atl_Check_6	GCTGCTAAACCTGCAGCTC	This study
Atl_Check_7	CAGTTGCTGCAAACAATG	This study
Atl_Check_8	CTGCTAAACCTGCAGCTC	This study
Atl_Check_9	AACGCATTCGTACATGCATTTG	This study
Atl_Check_10	CGCATTCGTACATGCATTTG	This study
Atl_Check_11	CTAACGGTAAATTAGCATGG	This study
sgRNA_check_F	AAAAATATGAACactctatcattg	(9)
sgRNA_check_R	CGGTGCCACTTTTTCAAGTT	(9)

PrimerA_Spa	TCAGGAGCTCACGGTGGTTTGACTGTAG	This study
PrimerB_Spa	CATACAGGGGGTATTAATAAACAAACAATACACAACG	This study
PrimerC_Spa	CGTTGTGTATTGTTTGTTTATTAATACCCCCTGTATG	This study
PrimerD_Spa	TCAGGTCGACGTAGAATTCACAATTCTAGC	This study
PrimerA_Sbi	TCAGGAGCTCAGACATGCGTTGAACCAC	This study
PrimerB_Sbi	GAGAAGATATTTTTGATTGAGTGTATTCCCTTTCTTTTTAC	This study
PrimerC_Sbi	GTAAAAAGAAAGGGAATACACTCAATCAAAAATATCTTCTC	This study
PrimerD_Sbi	TCAGGTCGACTAATCGTTTGCTAGTAATG	This study
pJB38_Fwd_NEW	GGGTTCCGCGCACATTTC	This study
pJB38_Rvs_NEW	TAAGGGTAACTAGCCTCGC	This study
Oligonucleotides used in this study		
AmiA Oligo	T*A*C*T*TC CCT AAA TAC GCA TAC CGT AAC GGC GTt GGg aGa CCc GAA GGg ATC GTt GTa gcc GAT ACA GCT AAT GATCGT TCG ACG ATA AAT	This study
NAGase Oligo	A*T*G*T*AT GGC ATT AAT GAA GTT TAT CTT ATC TCg CAc GCt t]Tg TTA Gcg ACg GGc AAt GGg ACT TCT CAA TTA GCG AAA GGT GCA GAT GTA	This study
sgRNA_AmiA_Up	**AGCTC** TC ATG AAC TAC GAT ACC TTC **G**	This study
sgRNA_AmiA_Down	**AAAAC** GAA GGT ATC GTA GTT CAT GA **G**	This study
sgRNA_NAGase_Up	**AGCTC** ACC GTT ACC TGT TTC TAA T **G**	This study
sgRNA_NAGase_Down	**AAAAC** TA TTA GAA ACA GGT AAC GGT **G**	This study

*, phosphodiester bonds; Lower case letters, altered bases for CRISPR counterselection; BOLD, *BsaI* cut site.

References

1. M. Nega, P. M. Tribelli, K. Hipp, M. Stahl, F. Götz, New insights in the coordinated amidase and glucosaminidase activity of the major autolysin (Atl) in *Staphylococcus aureus*. *Commun Biol* **3**, 695 (2020).

2. P. D. Fey, *et al.*, A genetic resource for rapid and comprehensive phenotype screening of nonessential *Staphylococcus aureus* genes. *mBio* **4,** e00537-12 (2013).

3. M. I. Goncheva, *et al.*, Stress-induced inactivation of the *Staphylococcus aureus* purine biosynthesis repressor leads to hypervirulence. *Nat. Commun.* **10**, 775 (2019).

4. L. E. Petrie, A. C. Leonard, J. Murphy, G. Cox, Development and validation of a high-throughput whole-cell assay to investigate Staphylococcus aureus adhesion to host ligands. *J. Biol. Chem.* **295**, 16700-16712 (2020).

5. D. Nair, *et al.*, Whole-genome sequencing of *Staphylococcus aureus* strain RN4220, a key laboratory strain used in virulence research, identifies mutations that affect not only virulence factors but also the fitness of the strain. *J. Bacteriol.* **193**, 2332–2335 (2011).

6. I. R. Monk, T. J. Foster, Genetic manipulation of Staphylococci-breaking through the barrier. *Front. Cell. Infect. Microbiol.* **2**, 49 (2012).

7. I. R. Monk, J. J. Tree, B. P. Howden, T. P. Stinear, T. J. Foster, Complete bypass of restriction systems for major *Staphylococcus aureus* Lineages. *mBio*. 6, e00308–15 (2015).

8. J. L. Bose, P. D. Fey, K. W. Bayles, Genetic tools to enhance the study of gene function and regulation in *Staphylococcus aureus*. *Appl. Environ. Microbiol.* **79**, 2218–2224 (2013).

9. K. Penewit, *et al.*, Efficient and scalable precision genome editing in *Staphylococcus aureus* through conditional recombineering and CRISPR/Cas9-mediated counterselection. *mBio* **9**, e00067-18 (2018).

10. R. M. Corrigan, T. J. Foster, An improved tetracycline-inducible expression vector for *Staphylococcus aureus*. *Plasmid* **61**, 126–129 (2009).